Using machine learning to dissect host kinases required for *Leishmania* internalization and development

Ling Wei[1], Umaru Barrie[2,3], Gina M. Aloisio[2,3,#], Francis T. H. Khuong[3,^], Nadia Arang[1,@], Arani Datta[3], Alexis Kaushansky[1,4,5,*], and Dawn M. Wetzel[3,6,*]

[1]Center for Global Infectious Disease Research, Seattle Children's Research Institute, Seattle, WA 98109, United States

[2]Medical Scientist Training Program, UT Southwestern Medical Center, Dallas, TX 75390, United States

[3]Department of Pediatrics, UT Southwestern Medical Center, Dallas, TX 75390, United States

[4]Department of Pediatrics, University of Washington, Seattle, WA 98105, United States

[5]Department of Global Health, University of Washington, Seattle, WA 98105, United States

[6]Department of Biochemistry, UT Southwestern Medical Center, Dallas, TX 75390, United States

Current addresses: [#]Department of Pediatrics (Emergency Medicine), Baylor College of Medicine, Houston, TX 77030; ^Medical Scientist Training Program, Texas Tech University, Lubbock, TX 79430; [@]Quantitative Biosciences Institute, School of Pharmacy, University of California San Francisco, San Francisco, CA 94143

*Corresponding authors. E-mail addresses: alexis.kaushansky@seattlechildrens.org (A. Kaushansky), dawn.wetzel@utsouthwestern.edu (D. M. Wetzel)

Keywords: *Leishmania*; phagocytosis; complement receptor; Fc receptor; kinase regression; phosphosignaling

Abstract

The *Leishmania* life cycle alternates between promastigotes, found in the sandfly, and amastigotes, found in mammals. When an infected sandfly bites a host, promastigotes are engulfed by phagocytes (*i.e.*, neutrophils, dendritic cells, and macrophages) to establish infection. When these phagocytes die or break down, amastigotes must be re-internalized to survive within the acidic phagolysosome and establish disease. To define host kinase regulators of *Leishmania* promastigote and amastigote uptake and survival within macrophages, we performed an image-based kinase regression screen using a panel of 38 kinase inhibitors with unique and overlapping kinase targets. We also targeted inert beads to complement receptor 3 (CR3) or Fcγ receptors (FcR) as controls by coating them with complement/C3bi or IgG respectively. Through this approach, we identified several host kinases that regulate receptor-mediated phagocytosis and/or the uptake of *L. amazonensis*. Findings included kinases previously implicated in *Leishmania* uptake (such as SRC family kinases (SFK), Abl family kinases (ABL1/c-Abl, ABL2/Arg), and spleen tyrosine kinase (SYK)); we also uncovered many novel kinases. These methods also predicted kinases necessary for promastigotes to convert to amastigotes or for amastigotes to survive within macrophages. Overall, our results suggest that the concerted action of multiple interconnected networks of host kinases are needed over the course of *Leishmania* infection, and that the kinases required for the parasite's life cycle substantially differ depending on which receptors are bound and the life cycle stage that is internalized. In addition, using our screen, we identified kinases that preferentially regulate the uptake of parasites over beads, indicating that the methods required for *Leishmania* to be internalized by macrophages differ significantly from generalized phagocytic mechanisms. Our findings are intended to be used as a hypothesis generation resource for the broader scientific community studying the roles of kinases in host-pathogen interactions.

49 **1. Introduction**

50 *Leishmania* is an obligate intracellular parasite of phagocytic cells that causes either
51 cutaneous or visceral disease, depending on the infecting parasite species and the
52 immunological status of the host [1, 2]. Since millions of patients are affected worldwide, and
53 drugs for leishmaniasis are both ineffective and have notable host toxicity, new anti-leishmanial
54 drugs are needed. Further research into the mechanisms driving *Leishmania* pathogenesis is
55 essential to identify new avenues for therapeutic development.

56 Targeting the process through which *Leishmania* is internalized by phagocytic cells
57 represents a potential therapeutic strategy. By blocking this process, the initial infection step
58 and subsequent spread of *Leishmania* within the host could be prevented. To this end, several
59 host cell receptors on macrophages have previously been identified as critical in *Leishmania*
60 binding, internalization, and subsequent survival within host cells [3]. As described in the
61 literature, the fibronectin receptor (integrin $\alpha5\beta1$) [4], mannose receptor [5], third complement
62 receptor CR3 [6], and first complement receptor CR1 [7] facilitate promastigote identification.
63 Additionally, CR3, heparin binding protein, and the Fc receptor (FcγR) mediate amastigote
64 recognition [8]. Ligation of these specific receptors is known to elicit downstream activation of
65 signaling pathways necessary for phagocytosis; however, the exact mechanisms of how
66 *Leishmania* modulates these signaling pathways and their contribution to the phagocytosis
67 process have yet to be elucidated.

68 Our ongoing efforts have been directed at identifying the host cell signaling pathways that
69 permit *Leishmania* internalization by mammalian macrophages. To this end, we have employed
70 a multi-color immunofluorescence assay to define *L. amazonensis* promastigotes or
71 amastigotes that have been internalized by, or are surviving within, macrophages [9, 10]. By
72 directing subsequent experiments at known signaling partners of previously-identified kinases in
73 other biological systems, we have defined a Src-Abl/Arg-Syk related signaling pathway that

74 governs *Leishmania* uptake and resulting disease manifestations in mouse models [10-13].
75 Such studies have been fruitful but are limited by what is known about interactions with each
76 identified kinase in other systems. Therefore, using a broader yet systematic screening
77 approach would provide a more complete picture of the signaling pathways used by *Leishmania*
78 to enter and survive in macrophages.

79 We have previously used a machine learning approach named kinase regression (KiR) to
80 identify host kinases responsible for malaria liver-stage infection [14], blood-brain barrier
81 integrity [15, 16] and dengue infection in hepatocytes [17]. By incorporating cellular phenotypic
82 data from a small panel of kinase inhibitors with existing biochemical data of these inhibitors
83 against 291 human protein kinases, KiR can make predictions on the key kinase regulators
84 driving that phenotype using an elastic net regularization algorithm [18].

85 Therefore, in this study, we used KiR to identify the most important host kinase regulators of
86 *L. amazonensis* uptake and development. A subset of these predictions was empirically
87 confirmed. Collectively, our predictions have identified important host cell regulators of *L.*
88 *amazonensis* infection, which vary depending on the entry receptor and form of the parasite.
89 These findings are shared here for the broader parasitology community and offer promising
90 insights into defining effective host-based targets for antiparasitic treatment.
91

92 **2. Materials and methods**

93 2.1 Mice

94 C57BL/6 mice were purchased from Jackson Laboratory (Bar Harbor, ME). The Institutional
95 Animal Care and Use Committee at UT Southwestern approved all experimental protocols.

96 2.2 Cell culture

97 For the initial kinase screen, cells were harvested from the tibias and femurs of mice and
98 differentiated into bone-marrow-derived (BM) primary macrophages over 7 days by growing
99 them in DMEM supplemented with 10% FBS and 20% supernatant from L929 cells.
100 Differentiation into BM macrophages was confirmed previously by fluorescence-activated cell
101 sorter (FACS) using antibodies to F4/80 and C11b (eBioscience, San Diego, CA); over 98% of
102 differentiated cells were positive for both markers. For confirmation screens with trametinib,
103 RAW 264.7 cells, a murine macrophage-like cell line, were used.

104 2.3 Parasite culture

105 *Leishmania amazonensis* promastigotes (strain MHOM/BR/767/LTB0016) were grown at
106 26°C in Schneider's Drosophila medium supplemented with 15% heat-inactivated, endotoxin-
107 free FBS and 10 μg/ml gentamicin. For macrophage invasion, promastigotes were incubated at
108 stationary phase for 7 days to maximize infective metacyclic promastigotes. *L. amazonensis*
109 amastigotes were grown axenically (outside of macrophages) at 32°C in M199 (Invitrogen) at
110 pH 4.5 supplemented with 20% FBS, 1% penicillin-streptomycin, 0.1% hemin (25 mg/ml in 50%
111 triethanolamine), 10 mM adenine, 5 mM L-glutamine, 0.25% glucose, 0.5% Trypticase, and 40
112 mM sodium succinate.

113 2.4 Phagocytosis assays

114 Primary macrophages were incubated overnight in M-CSF-starved media. One hour prior to
115 phagocytosis, macrophages were activated with PMA (Sigma) for 1 h. Experiments were

116 performed at ~50% confluence. For drug screening experiments, macrophages were
117 preincubated in 500 nM of each kinase inhibitor or DMSO (Sigma) for 2 h. For experiments with
118 C3bi-opsonized particles, 2-μm-diameter latex yellow-green beads (Sigma) were coated with
119 human IgM (Sigma) at 1:100 for 1 h at 37°C. They were then incubated in freshly isolated
120 mouse serum diluted 1:2 in phosphate-buffered saline (PBS) for 1 h at 37°C, which allowed
121 C3bi opsonization. For IgG experiments, beads were incubated with rabbit IgG (Sigma) diluted
122 1:250 for 1 h at 37°C. Macrophages were incubated with a ratio of 10 to 15 particles per cell for
123 the indicated timepoints at 37°C. For survival assays of 24 and 72 h, macrophages were
124 washed with fresh media and then given fresh media to remove any beads that had not been
125 taken up. Coverslips were rinsed, fixed with 3% paraformaldehyde for 15 min, and blocked with
126 2% bovine serum albumin (BSA) without permeabilization. Coverslips with C3bi-coated beads
127 were incubated with rabbit anti-human IgM (Sigma) at 1:250. All coverslips were labeled with
128 A568-conjugated goat anti-rabbit secondary antibody (Invitrogen) at 1:250. Coverslips were
129 permeabilized with 0.25% Triton for 10 min, and stained with DAPI (4′,6-diamidino-2-
130 phenylindole) (Invitrogen). This process, termed a “three-color immunofluorescence assay”,
131 allowed us to distinguish the beads that were internalized from those that remained outside
132 cells. As experiments were performed in 96 well plates, 25% formaldehyde was added directly
133 to wells to make a final dilution of 3% formaldehyde, and cells were again fixed for 15 min. The
134 experiment then proceeded as listed above.

135 2.5 *Leishmania* uptake assays

136 Primary mouse bone marrow-derived macrophages were employed for all assays.
137 Macrophages were grown on black 96-well plates and were incubated with 500 nM kinase
138 inhibitors (screening assays) or 1 μM trametinb (confirmation assays) for 2 h prior to parasite
139 addition. Macrophages were also activated with PMA for 1 h prior to experiments. For C3bi
140 opsonization experiments, promastigotes and amastigotes were incubated with freshly isolated

141 mouse serum for 1 h. For IgG opsonization, amastigotes were coated with anti-P8–
142 proteoglycolipid complex (monoclonal antibody IgG1) for 1 h. Because promastigotes are
143 unlikely to encounter specific antibodies during an animal infection (it is not a biologically
144 relevant condition if an animal has not been previously infected), IgG opsonization of
145 promastigotes was not performed. Promastigotes were incubated at a ratio of 10 parasites : 1
146 macrophage and amastigotes were incubated at a ratio of 5 parasites : 1 macrophage. For
147 experiments performed in 96-well plates, 25% formaldehyde was added directly to wells to
148 make a final dilution of 3% paraformaldehyde. External promastigotes were labeled with mouse
149 anti-gp46, while external amastigotes were labeled with mouse anti-P8. All coverslips and plates
150 were labeled with A594-conjugated goat anti-mouse secondary antibody (Invitrogen). After
151 permeabilization, promastigotes were relabeled with mouse anti-gp46, and amastigotes were
152 relabeled with mouse anti-P8 and A488-conjugated goat anti-mouse secondary antibody
153 (Invitrogen); samples were co-stained with DAPI. For all experiments, at least 10 randomly
154 selected, distinct fields were visualized containing at least 100 macrophages and at least 100
155 parasites per experimental determination. All experiments were performed 3 times unless
156 otherwise indicated.

157 2.6 Parasite survival assays

158 For parasite survival assays, macrophages were treated as above, except longer timepoints
159 of 24 h and 72 h were employed. At the 24 h mark, cells were washed with media, and fresh
160 media was given. For experiments on coverslips, macrophages were fixed with 3%
161 paraformaldehyde and for experiments performed in 96-well plates, 25% formaldehyde was
162 added directly to wells to make a final dilution of 3% paraformaldehyde. After permeabilization,
163 promastigotes had switched to amastigotes based on morphological changes and binding of
164 amastigote-specific antibodies, and amastigotes were labeled with mouse anti-P8 and A488-
165 conjugated goat anti-mouse secondary antibody (Invitrogen); samples were co-stained with

166 DAPI. For all experiments, at least 10 randomly selected, distinct fields were visualized
167 containing at least 100 macrophages and at least 100 parasites per experimental determination.
168 All experiments were performed 3 times unless otherwise indicated.

169 2.7 Microscopy

170 For the initial kinase screen, fluorescence was visualized in the UT Southwestern High
171 Throughput Screening Core on a InCell Analyzer 6000 (GE Healthcare Life Sciences) at 20X. At
172 least 10 randomly selected fields from multiple technical replicates were visualized for a total of
173 at least 100 macrophages per experimental determination. The mean phagocytic index (PI), the
174 number of particles internalized per 100 mammalian cells, was calculated for each experiment
175 using a pipeline from CellProfiler (https://cellprofiler.org, Broad Institute). The phagocytic index
176 for control cells was taken as the maximum value (100%) for each experiment. Means ±
177 standard errors (SE) were calculated, and each biological experiment was performed at least
178 three times. One-sample Student's *t* tests were performed to assess statistical significance.
179 Confirmation assays using trametinib were performed similarly, except that samples were
180 visualized on a Cytation 5 (BioTek), and analysis was performed using the system's automated
181 software [12].

182 2.8 Kinase regression

183 The elastic net regularization algorithm used for this study was published previously [15].
184 The kinase regression (KiR) approach exploits the polypharmacology of a small panel of kinase
185 inhibitors and makes predictions on kinases important for specific cellular phenotypes and the
186 effect of untested kinase inhibitors on the phenotypes based on the linear combination of the
187 contributions of kinases to the phenotypes [18]. For this study, the mean number of internal
188 parasites per 100 mammalian cells upon kinase inhibitor treatment was normalized to the
189 phagocytic index upon DMSO treatment as control. The normalized phagocytic indices, together
190 with the biochemical data of the panel of 38 kinase inhibitors against 300 recombinant protein

191 kinases, were input into the elastic net regularization algorithm with a condition-specific cross-
192 validation strategy. The glmnet package (https://github.com/bbalasub1/glmnet_python, version
193 2.2.1) in Python (https://www.python.org, version 3.7.6) was used to perform elastic net
194 regularization, with the elastic net mixing parameter of 0.8.

195 2.9 Network generation

196 To build the phosphosignaling network for a set of KiR-predicted kinases, the shortest paths
197 between any pair of kinases within that set was identified using the kinase-substrate
198 phosphorylation database on PhosphoSitePlus® as the background network, and all the paths
199 were combined to form the phosphosignaling network that describes the paths through which
200 the signals may propagate. Searches for the shortest paths between kinases were done using
201 NetworkX (https://github.com/networkx/networkx), a Python package for analyzing complex
202 network structures.

203 2.10 Visualization

204 Schematics were created with BioRender.com. Phosphosignaling networks were visualized
205 using Cytoscape (https://cytoscape.org, version 3.9.1), with the hierarchic layout from yFiles
206 layout algorithms (https://www.yworks.com/products/yfiles-layout-algorithms-for-cytoscape).

207

208 **3. Results**

209 3.1 A broad-scale, overlapping-target kinase inhibitor screen implicates many host cell
210 kinases in *Leishmania* uptake of macrophages and intracellular development

211 *Leishmania* infection of macrophages can be initiated with promastigotes, the form
212 developed in the female sandfly's digestive tract, or with amastigotes that replicate within
213 phagolysosomes of mammalian host cells [19]. We can also grow *L. amazonensis* amastigotes
214 in the laboratory outside of host cells (axenically) in rich, low pH media. As indicated above,
215 multiple surface protein receptors, including complement receptor CR3, facilitate promastigote
216 uptake; both CR3 and Fc receptor (FcR) permit amastigote uptake [20, 21]. We hypothesized
217 that if *Leishmania* promastigotes and amastigotes bound different extracellular receptors prior to
218 internalization, these receptors might influence the signaling pathways facilitating parasite
219 uptake by and survival within macrophages. To test this hypothesis and study the effects of
220 binding different receptors, we cultured *L. amazonensis* promastigotes and axenic amastigotes
221 [10, 20, 21]; promastigotes were opsonized with C3bi and amastigotes were coated with C3bi or
222 IgG (Fig. 1A). We did not coat promastigotes with IgG because antibody opsonization of
223 promastigotes is unlikely to be physiologically relevant (unless a host organism were infected
224 with *Leishmania* parasites multiple times). We simultaneously pre-treated bone marrow-derived
225 macrophages with a panel of 38 kinase inhibitors to probe for kinase regulators responsible for
226 *Leishmania* uptake and intracellular development. Four different co-incubation timepoints were
227 employed to broadly characterize *Leishmania* uptake into and survival within macrophages: 0.5
228 hour for initial parasite uptake, 3 hours to encapsulate the end of parasite uptake and trafficking
229 to the parasitophorous vacuole (PV), 24 hours to demonstrate transition from promastigote to
230 amastigote forms, and 72 hours to assess intracellular replication of amastigotes (Fig. 1B).
231 Hence, we exposed coated promastigotes and amastigotes to macrophages at a ratio of 10:1
232 and 5:1, respectively, for 0.5, 3, 24 and 72 hours before fixation with formaldehyde. We then

233 processed samples for immunofluorescence without permeabilization so that extracellular and
234 intracellular parasites could be differentiated. In brief, external promastigotes were labeled with
235 mouse anti-gp46 antibody and external amastigotes were labeled with mouse anti-P8 antibody,
236 followed by secondary staining with A568-conjugated goat anti-mouse secondary antibody (Fig.
237 1C). After permeabilization, parasites were visualized by labeling promastigotes with mouse
238 anti-gp46 antibody or amastigotes with mouse anti-P8 antibody followed by secondary staining
239 with A488-conjugated goat anti-mouse secondary antibody (Fig. 1C). We found that our 38
240 screened kinase inhibitors had a diverse impact on *Leishmania* uptake and development in
241 macrophages at different timepoints, life cycle stages, and when parasites had bound different
242 cell surface receptors (Fig. 1D, Table S1).

243 3.2 *Leishmania* uptake and intracellular development is differentially impacted by host
244 kinases depending upon life cycle stage and the entry receptor

245 To examine how inhibition of various kinases varied outcomes under different entry
246 conditions, we assessed correlations of phagocytic indexes across the panel of 38 kinase
247 inhibitors between amastigote uptake via CR3 and FcR, and between promastigote and
248 amastigote uptake via CR3. We observed little association (r: 0.14 – 0.31) between the
249 inhibition of C3bi- and IgG- mediated entry mechanisms (Fig. 1E, top), and also, little correlation
250 (r: -0.066 – 0.20) between promastigote and amastigote forms entering macrophages via a
251 C3bi-mediated mechanism (Fig. 1E, bottom). The lack of correlation between these different
252 scenarios suggested that different kinase regulators and kinase signaling pathways control
253 *Leishmania* invasion via different entry mechanisms, and furthermore, that even if they employ
254 the same entry mechanisms, different life cycle stages of *Leishmania* require different sets of
255 kinase regulators and kinase signaling for successful invasion and development in
256 macrophages.

3.3 Kinase regression predicts that kinases required for *Leishmania* infection of macrophages can either overlap or diverge from kinases implicated in phagocytosis of coated, inert beads

In the past, there had been a prevailing belief in the *Leishmania* research community that early signaling events involved in *Leishmania* internalization closely resemble generalized phagocytic mechanisms [7, 22]. This belief has largely stemmed from older studies that focused on host cell responses to cytoskeleton-active agents [7]. This hypothesis contrasts with other intracellular parasites such as *Toxoplasma* and *Trypanosoma cruzi*, where cell invasion is predominantly reliant on parasitic machinery [22]. However, this historical belief has been evolving over time. Given the unique pattern of kinase inhibitor effects observed across different entry mechanisms and parasite forms (Fig. 1D, E), we hypothesized that distinct kinase regulatory processes would regulate C3bi or IgG-opsonized bead uptake (generalized phagocytosis) compared to promastigote or amastigote infection (*Leishmania* internalization). Therefore, next, we sought to understand the similarities and differences between the kinase regulatory program governing host control of *Leishmania* infection and the mechanisms that regulate phagocytosis in general.

To understand the core kinases that control *Leishmania* invasion and development in macrophages, we used a machine learning approach called kinase regression (KiR), which utilizes the kinase screen data on *Leishmania* infection along with existing biochemical data of these kinase inhibitors against 291 human kinases [23] to make predictions on the kinases important for the phenotype of interest (Fig. 2A). In addition to making predictions on kinase regulators, KiR also predicts the effect of untested kinase inhibitors in the screen on *Leishmania* infection for inhibitors with biochemical data available. For each experimental condition, KiR was performed on the data taken at the respective stages of infection. Known and novel kinase regulators were predicted to modulate *Leishmania* invasion and intracellular development. A full

282 list of kinases predicted to facilitate or inhibit bead and *L. amazonensis* uptake and persistence
283 are shown in Table S2.

284 To study if and how the mechanism of *Leishmania* uptake by macrophages is different from
285 phagocytosis, as well as how signaling events change over time for this intracellular parasite,
286 we compared KiR predictions between *Leishmania* and bead uptake by, and persistence within,
287 macrophages. We reasoned that three distinct options were feasible. (1) If early infection was
288 mediated strictly by host regulators of phagocytosis, we would observe a high degree of overlap
289 in kinases predicted to regulate C3bi-coated bead versus parasite uptake and IgG-coated bead
290 versus amastigote uptake, which would then diverge as parasites changed their host
291 requirements at later (survival) time points. (2) In contrast, if significant overlap existed
292 throughout infection at both early and late timepoints, we reasoned that phagocytic uptake
293 would intrinsically shape the host regulators of infection throughout the process. (3) Finally, if
294 little overlap in host kinases for parasites versus beads were present early on during infection,
295 we reasoned that distinct mechanisms would dominate entry.

296 Interestingly, for the three parasite uptake mechanisms we tested and compared to bead
297 uptake, we observed examples of all three patterns described above. Kinase predictions of IgG-
298 mediated amastigote and bead uptake suggested modest overlap through the entire parasite
299 lifecycle at early and late time points (Fig. 2B), most similar to model (2) above. Despite this,
300 most KiR-predicted kinases were unique to amastigote + IgG infection throughout the time
301 course. Interestingly, when comparing promastigotes and beads, both treated with C3bi, we
302 observed less overlap between the two lists of kinase predictions than would be predicted by
303 chance (Fig. 2C). We interpret this finding to suggest that C3bi-promastigotes have largely
304 unique kinase regulatory requirements from beads that enter strictly by phagocytosis, more
305 similar to the model described in point (3) above. Finally, and perhaps most strikingly, we saw a
306 dramatic similarity in the overlap between kinases predicted to regulate early time points of

307 amastigotes and beads treated with C3bi. This overlap waned as time progressed, most similar
308 to model (1) above (Fig. 2D). The significant overlap of kinase regulators between C3bi-
309 amastigote and bead uptake suggested that internalization of amastigotes via a C3bi-mediated
310 mechanism is more phagocytosis-driven than other methods. However, once an amastigote
311 successfully invades macrophages, non-phagocytic-associated signaling becomes essential for
312 its intracellular development. These results suggested that the mechanism and receptor driving
313 the initial uptake of *Leishmania* parasites often but does not always influence its ultimate cellular
314 fate, which is consistent with a subset of prior literature [7, 24].

315 3.4 Additional kinase regression analysis predicts that several kinases are required for
316 both *Leishmania* infection of macrophages and phagocytosis

317 To better understand the portion of network-level kinase signaling that overlapped with
318 phagocytosis during *Leishmania* infection, we built phosphosignaling networks from the
319 predicted kinases overlapping between *Leishmania* and bead uptake conditions, using the
320 kinase-substrate phosphorylation database on PhosphoSitePlus® as the background network
321 (Fig. 2E). PhosphoSitePlus® is a dynamically updated knowledgebase that integrates both low-
322 and high-throughput data sources into a single reliable and comprehensive resource for
323 studying experimentally observed post-translational modifications in the regulation of biological
324 processes [25]. These kinase phosphosignaling networks revealed many additional kinases that
325 were not predicted by KiR but were predicted to serve as intermediates, connecting KiR-
326 predicted kinases. For instance, at 3 h of infection where amastigotes have finished internalizing
327 into the cell and start trafficking to PV, the model predicted that MAPK signaling plays an
328 important role in amastigote-initiated uptake as well as IgG-bead uptake (Fig. 2E). As further
329 evidence of the importance of MAPK in early phagocytosis and *Leishmania* infection, a
330 canonical MAPK signaling architecture (MAP3K-MAP2K-MAPK) was also implicated in the
331 network built from the kinases shared between promastigote and bead uptake via a C3bi-

332 mediated mechanism at 3 h of infection (Fig. S2A). Similarly, another canonical MAPK signaling
333 architecture, MAP2K-MAPK-MAPKAPK, was inferred by the network built from the shared
334 kinases between promastigote and bead uptake at the early stage of invasion (Fig. S2B). To
335 experimentally evaluate these predictions, we assessed infection of macrophages by IgG-
336 opsonized amastigotes and IgG-coated beads at multiple timepoints in the presence of
337 trametinib, a MEK (MAP2K) inhibitor (3 h data shown in Fig. 2F; additional timepoints and
338 promastigotes can be found in [13]). Overall, our network analysis suggests that a subset of
339 phagocytic pathways is required for *Leishmania* infection. However, there are more non-
340 phagocytic-associated signaling pathways essential for establishing *Leishmania* infection in
341 macrophages, which are analyzed further in the following sections.

342 3.5 Both differential and overlapping kinase signaling pathways are predicted to be
343 associated with amastigote versus promastigote infection of macrophages

344 Both *Leishmania* promastigotes (insect stage) and amastigotes (mammalian stage) can be
345 internalized by macrophages. Promastigotes and amastigotes differ in their morphology,
346 proteomes, and membrane constituents. Given the distinct origins and characteristics of these
347 two parasite life cycle stages, it is reasonable to hypothesize that different sets of host kinase
348 regulators are involved in the uptake and subsequent regulation of parasite survival within the
349 host cell. Our KiR model indeed predicted the involvement of different kinases for promastigote
350 invasion into macrophages compared to amastigotes, including several novel kinases not
351 previously implicated in *Leishmania* infection and kinases unrelated to phagocytosis (Fig. 3A).
352 Interestingly, a small set of kinases were predicted to be important for intracellular development
353 for both promastigotes and amastigotes via a C3bi-mediated entry mechanism, and this overlap
354 was statistically significant compared to random selections from the pool of 291 kinases in the
355 screen (Fig. 3A). Since promastigotes transition to amastigotes forms approximately 24 h after
356 macrophage infection, the increased overlap of predicted kinases between promastigote- and

357 amastigote-initiated infection at 24 h and 72 h post-infection may be attributed to this transition
358 within macrophages at later infection stages. Nonetheless, the significant number of kinases
359 predicted to be uniquely essential for promastigote- or amastigote-initiated infection suggests
360 that distinct kinase signaling pathways regulate the establishment of *Leishmania* parasites in
361 macrophages during and after life cycle stage conversion.

362 To further capture the molecular details of kinase signaling that are unique to promastigote-
363 initiated infection, we built phosphosignaling networks from KiR-predicted kinases unique to the
364 uptake of promastigotes but not uptake of amastigotes or beads via a C3bi-mediated entry
365 mechanism. For example, at 24 h post infection, when internalized promastigotes transition to
366 amastigotes, MAPK signaling was once again enriched in the phosphosignaling network built
367 from kinases predicted to exclusively regulate promastigote-initiated infection, with 12 out of 58
368 kinases in this network belonging to the MAP kinase family (Fig. 3B, hypergeometric test p-
369 value of 0.0046). This pathway analysis suggests that different kinase signaling pathways are
370 required for establishing promastigote- and amastigote-initiated infection in macrophages, which
371 is consistent with some prior literature characterizing differences between these [7].

372 3.6 Differential kinase signaling is predicted to drive C3bi- versus IgG-mediated *Leishmania*
373 uptake and survival versus that of coated inert beads

374 The uptake of *Leishmania* parasites is facilitated by various host cell surface protein
375 receptors, such as complement receptors and Fc receptors, and different parasite forms
376 primarily interact with different receptors for their successful invasion [6-8]. As suggested in
377 section 3.3, binding different receptors may trigger different downstream host signaling
378 pathways that regulate *Leishmania* survival and intracellular development. For example, *L.*
379 *amazonensis* binding to CR3 is known to trigger Rho GTPase recruitment and cytoskeletal
380 rearrangement. Phagocytic vesicles formed post-CR3-mediated uptake exhibit a snug fit, and
381 phagolysosome maturation is delayed, which accompanies impaired accumulation of LAMP-1

382 and cathepsin-D. CR3 binding also hampers IFN-γ-induced pro-inflammatory signaling and
383 reduce IL-12-mediated H_2O_2 production [7]. Conversely, when *Leishmania* binds FcR, it triggers
384 Rac GTPase recruitment and cytoskeletal rearrangement. Rac, in turn, activates NADPH
385 oxidase, and the resulting phagocytic vesicles formed after FcR-mediated uptake are expansive.
386 However, the kinases that govern *Leishmania* uptake and survival based on differential
387 opsonization are less well described, although some studies do exist in the literature; for
388 example, IgG opsonization of amastigotes has been shown to modulate Rac-1 activation during
389 uptake [24].

390 Thus, we next inquired if differential kinase signaling would mediate C3bi- versus IgG-
391 mediated amastigote uptake and survival. Comparing the KiR-predicted kinase regulators
392 between C3bi- and IgG-amastigotes during infection, we observed limited overlap in the
393 regulatory kinases predicted in each condition (Fig. 4A). In fact, overlap between predicted
394 regulatory kinases at 3 and 24 h post-infection exhibited a higher number of kinases than
395 predicted by chance alone. These KiR predictions support the hypothesis that the uptake of
396 amastigotes through a C3bi-mediated mechanism engages a different set of host kinases
397 compared to those regulating entry through an IgG-mediated mechanism. Moreover, distinct
398 sets of host kinases are likely required for the subsequent intracellular replication of *Leishmania*.
399 Furthermore, we considered the possibility that the uptake of *Leishmania* may necessitate host
400 kinase signaling pathways distinct from those regulating phagocytosis. Therefore, we utilized
401 our data to identify regulatory factors essential exclusively for *L. amazonensis* infection. To
402 achieve this, we initially compared our KiR-predicted kinase regulators between C3bi- and IgG-
403 mediated uptake of inert beads as controls (Fig. 4B). As anticipated, akin to the uptake of
404 amastigotes, distinct sets of kinases were implicated in regulating C3bi- and IgG-mediated
405 phagocytosis, with the most pronounced differences observed during the initial uptake phase
406 (0.5 h) between these two phagocytic pathways (Fig. 4B). We then built phosphosignaling

407 networks from KiR-predicted kinases that were unique to uptake of amastigotes via a C3bi-
408 mediated mechanism, but were not involved in either of the phagocytosis pathways. In addition
409 to MAPK signaling pathways, multiple other kinase-kinase connections were implicated in the
410 network built during initial uptake (0.5 h) (Fig. 4C). For instance, network analysis suggested
411 that AKT serine/threonine kinase 1 (AKT1) and glycogen synthase kinase 3 beta (GSK3B)
412 signaling is important for amastigote-initiated infection via a C3bi-mediated mechanism.
413 Interestingly, previous studies have shown that activation of GSK3B suppresses IL-10
414 production for a protective immune response against *Leishmania* infection [26, 27]. Our model
415 also predicted that SRC-mediated signaling associated with transforming growth factor beta
416 receptor (TGF-βR) is essential for uptake of amastigotes via binding to complement receptors.
417 Consistent with this prediction, both field and *in vitro* studies conducted by others have reported
418 that TGF-βRs are involved in *Leishmania* infection, although these were done with different
419 *Leishmania* strains other than *L. amazonensis* [28, 29]. Overall, our results demonstrate the
420 potential of using KiR and network-level analysis to systematically dissect key kinase regulators
421 and underlying signaling pathways associated with *Leishmania* infection.

422

423 **4. Discussion**

424 Here, we conducted an image-based kinase regression screen to define host kinase
425 regulators of *L. amazonensis* promastigote and amastigote uptake and survival within
426 macrophages. Furthermore, to define kinases required for general phagocytic mechanisms, we
427 coated inert beads with C3bi or IgG, respectively, to target them to CR3 or FcγR. Our findings
428 are presented as a tool for the scientific community to engender further studies of *Leishmania*
429 uptake by, and survival within, mammalian macrophages. Our approach identifies several host
430 kinases that regulated receptor-mediated phagocytosis and/or the uptake of *Leishmania*. In
431 addition, we delineate kinases necessary for promastigotes to convert to amastigotes or for
432 amastigotes to survive within macrophages. Our data demonstrate that the host kinases
433 required for these processes differ depending on which *Leishmania* life cycle stage is
434 internalized and which cell surface receptors are bound. We also identify kinases that
435 preferentially regulate the uptake of parasites over opsonized beads, indicating that the
436 methods required for *Leishmania* to be internalized by macrophages differ substantially from
437 generalized phagocytic mechanisms.

438 The kinase regression approach has been successfully implemented in several other
439 biological systems to dissect key host kinase regulators important for phenotypes of interest.
440 KiR utilizes small-scale kinase inhibitor screens, along with known biochemical information on
441 the kinase inhibitors against hundreds of protein kinases, to make predictions on the kinases
442 regulating the cellular phenotypes screened for and on the impact of untested kinase inhibitors
443 on the phenotypes, simply through an elastic net regularization algorithm. Although our KiR
444 methodology does not consider factors such as protein abundance, subcellular localization,
445 translation, degradation, and dephosphorylation, which are all vital for comprehending cell
446 signaling driven by post-translational modifications, it provides the capability to connect kinases
447 with cellular phenotypes in an unbiased and systematic manner. In turn, this allows it to

448 elucidate the functionality of kinase regulators associated with particular phenotypes. By
449 building phosphosignaling networks, we expanded the scope from the 291 kinases in the
450 biochemical dataset used for KiR to the entire human kinome and connected functional kinases
451 within a network structure that describes the pathways through which the phosphosignals
452 propagate. Thus, our approach provides insights on the underlying kinase signaling
453 mechanisms controlling *Leishmania* uptake and intracellular development.

454 Established literature would suggest that *Leishmania* uptake by macrophages involves
455 generalized phagocytic mechanisms [7], even though this complex organism possesses
456 substantial structural and proteomic differences from other commonly-phagocytosed particles.
457 In our experiments, if early infection were mediated strictly by host regulators of phagocytosis,
458 we would predict that the kinases governing C3bi-coated promastigote/amastigote or IgG-
459 coated amastigote uptake would overlap significantly with similarly opsonized beads. However,
460 except for kinases predicted to regulate early time points of C3bi-amastigote and bead uptake,
461 we instead find that the kinases required for *Leishmania* IgG-opsonized amastigote and C3bi-
462 opsonized promastigote uptake by macrophages are predicted to be significantly different than
463 those required for phagocytosis of coated beads. Our ongoing studies presented here and
464 elsewhere have begun to experimentally validate this finding (*e.g.,* through inhibition of MAP
465 kinases, see [13]). Thus, our findings challenge prior hypotheses in the field and suggest that
466 further studies of the internalization process will not only uncover novel mechanisms for
467 *Leishmania* entry into macrophages, but could also suggest novel host-active agents that could
468 be specific to treat leishmaniasis.

469 Our studies implicate that host kinase signaling pathways change over time as *Leishmania*
470 parasites establish their intracellular niche, which has been demonstrated by others [7].
471 However, our data suggest that even signaling events that are related to parasite survival and
472 subsequent development taking place hours to days after internalization can be influenced by

473 the initial receptor that is bound. Our results both complement and add to prior literature
474 suggesting that activating different cell surface receptors on phagocytes affects the eventual
475 fate of this intracellular parasite.

476 In addition, we find that different life cycle stages of *L. amazonensis* trigger different host
477 kinase signaling events during their uptake by and survival within macrophages. Given the
478 remarkable differences between parasite size and composition in these two life cycle stages,
479 perhaps this is not altogether surprising. However, we simultaneously demonstrate that the host
480 macrophage receptor to which a *Leishmania* amastigote initially binds often affects later
481 signaling events while the parasite resides within the macrophage. For example, our predictions
482 of kinases required for IgG-mediated amastigote and bead uptake suggest modest overlap
483 through the entire parasite life cycle at early and late time points, which diverges from C3bi-
484 mediated amastigote uptake. We anticipate that in turn, these differential signaling pathways
485 would then affect the parasite's eventual fate and survival, which we will test directly in our
486 future work.

487 In conclusion, our studies implicate many host kinases in *L. amazonensis* promastigote and
488 amastigote internalization by macrophages as well as generalized phagocytosis. We have also
489 described host kinase signaling pathways seen while promastigotes convert to amastigotes
490 within the macrophage or are activated while *Leishmania* survives within the acidic
491 phagolysosome. Interestingly, there are many differences between the kinases that play roles in
492 *Leishmania* versus bead internalization, promastigote versus amastigote uptake and survival,
493 and CR3 versus FcR-activated pathways. As these mechanisms may also differ based on the
494 infecting species of *Leishmania*, further studies will be directed at identifying differences in
495 kinase signaling pathways between entry and survival of these life cycle stages in different
496 parasite species. Uncovering the kinases that control the internalization of *Leishmania* by

497 macrophages and its subsequent growth and development in phagocytes may lead to novel

498 host-based targets for new antimicrobials.

499

500 **Data availability**

501 Data generated in this study are available in the main text or the supplementary information.

502

503 **Acknowledgements**

504 We would like to thank members and colleagues of the Wetzel and Kaushansky laboratories for
505 technical assistance and helpful comments, including Laela M. Booshehri, James M. Bradford,
506 Lauren T. Callaghan, Ivan Luu, Emily T. Mamula, Emma L. Rhodes, Catherine Trice, and Imran
507 Ullah. Drs. Hanspeter Niederstrasser and Bruce A. Posner in the UT Southwestern High
508 Throughput Screening Core helped image the initial uptake and survival kinase inhibitor screen
509 with the Core's InCell Analyzer 6000, which was purchased through NIH S10 OD018005. This
510 work has been supported by NIH K08 AI103036, NIH R01 AI146349, Children's Clinical
511 Research Advisory Committee (CCRAC) Junior and Early Investigator Awards, a Welch Grant
512 for Chemistry (I-2086), and funds from the Department of Pediatrics (all to DMW), and NIH R01
513 GM101183 (to AK). UB and GA were supported by Medical Scientist Training (MD/PhD) Grant
514 NIH T32 GM008014. In addition, UB was funded by a National Institutes of Health Supplement
515 to Promote Diversity in Health-Related Research (R01 AI146349-S1).

516

517 **CRediT authorship contribution statement**

518 **Ling Wei:** Conceptualization, Investigation, Writing – Original Draft, Writing – Review & Editing.
519 **Umaru Barrie:** Investigation, Validation, Formal Analysis, Data Curation, Visualization, Writing
520 – Original Draft, Writing – Review & Editing. **Gina M. Aloisio:** Methodology, Validation,
521 Investigation, Formal Analysis. **Francis T. H. Khuong:** Validation, Formal Analysis, Data
522 Curation, Investigation, Writing – Review & Editing. **Nadia Arang:** Conceptualization, Formal
523 Analysis. **Arani Datta:** Validation, Formal Analysis, Data Curation, Investigation, Writing –

Review & Editing. **Alexis Kaushansky:** Conceptualization, Funding Acquisition, Supervision, Project Administration, Writing – Review & Editing. **Dawn M. Wetzel:** Conceptualization, Methodology, Formal Analysis, Resources, Funding Acquisition, Supervision, Project Administration, Writing – Original Draft, Writing – Review & Editing.

Declaration of Competing Interest

The authors declare that they have no competing interests.

532 **References**

533 1. Burza, S., S.L. Croft, and M. Boelaert, *Leishmaniasis.* Lancet, 2018. **392**(10151): p. 951-
534 970.
535 2. CDC. *Parasites - Leishmaniasis*. 2022; Available from:
536 https://www.cdc.gov/parasites/leishmaniasis/index.html.
537 3. Wenzel, U.A., et al., *Leishmania major parasite stage-dependent host cell invasion and*
538 *immune evasion.* FASEB J, 2012. **26**(1): p. 29-39.
539 4. Brittingham, A., et al., *Interaction of Leishmania gp63 with cellular receptors for*
540 *fibronectin.* Infect Immun, 1999. **67**(9): p. 4477-84.
541 5. Mosser, D.M. and L.A. Rosenthal, *Leishmania-macrophage interactions: multiple*
542 *receptors, multiple ligands and diverse cellular responses.* Semin Cell Biol, 1993. **4**(5):
543 p. 315-22.
544 6. Wilson, M.E. and R.D. Pearson, *Roles of CR3 and mannose receptors in the attachment*
545 *and ingestion of Leishmania donovani by human mononuclear phagocytes.* Infect Immun,
546 1988. **56**(2): p. 363-9.
547 7. Ueno, N. and M.E. Wilson, *Receptor-mediated phagocytosis of Leishmania: implications*
548 *for intracellular survival.* Trends Parasitol, 2012. **28**(8): p. 335-44.
549 8. Peters, C., et al., *The role of macrophage receptors in adhesion and uptake of Leishmania*
550 *mexicana amastigotes.* J Cell Sci, 1995. **108 (Pt 12)**: p. 3715-24.
551 9. Wetzel, D.M., et al., *Actin filament polymerization regulates gliding motility by*
552 *apicomplexan parasites.* Mol Biol Cell, 2003. **14**(2): p. 396-406.
553 10. Wetzel, D.M., D. McMahon-Pratt, and A.J. Koleske, *The Abl and Arg kinases mediate*
554 *distinct modes of phagocytosis and are required for maximal Leishmania infection.* Mol
555 Cell Biol, 2012. **32**(15): p. 3176-86.
556 11. Wetzel, D.M., et al., *The Src kinases Hck, Fgr, and Lyn activate Abl2/Arg to facilitate*
557 *IgG-mediated phagocytosis and Leishmania infection.* J Cell Sci, 2016. **129**(16): p. 3130-
558 43.
559 12. Ullah, I., et al., *Src- and Abl-family kinases activate spleen tyrosine kinase to maximize*
560 *phagocytosis and Leishmania infection.* J Cell Sci, 2023. **136**(14).
561 13. Barrie, U., et al., *ERK1/2 activation in macrophages promotes Leishmania*
562 *internalization and pathogenesis.* Accepted at Microbes and Infection; bioRxiv, 2022: p.
563 doi: 10.1101/2022.12.08.517760.
564 14. Arang, N., et al., *Identifying host regulators and inhibitors of liver stage malaria*
565 *infection using kinase activity profiles.* Nat Commun, 2017. **8**(1): p. 1232.
566 15. Dankwa, S., et al., *Exploiting polypharmacology to dissect host kinases and kinase*
567 *inhibitors that modulate endothelial barrier integrity.* Cell Chem Biol, 2021.
568 16. Wei, L., et al., *Interrogating endothelial barrier regulation by temporally resolved kinase*
569 *network generation.* Life Sci Alliance, 2024. **7**(5).
570 17. Bourgeois, N.M., et al., *Multiple receptor tyrosine kinases regulate dengue infection of*
571 *hepatocytes.* Front Cell Infect Microbiol, 2024. **14**: p. 1264525.
572 18. Gujral, T.S., L. Peshkin, and M.W. Kirschner, *Exploiting polypharmacology for drug*
573 *target deconvolution.* Proc Natl Acad Sci U S A, 2014. **111**(13): p. 5048-53.
574 19. Kane, M.M. and D.M. Mosser, *Leishmania parasites and their ploys to disrupt*
575 *macrophage activation.* Curr Opin Hematol, 2000. **7**(1): p. 26-31.

576 20. Russell, D.G. and S.D. Wright, *Complement receptor type 3 (CR3) binds to an Arg-Gly-*
577 *Asp-containing region of the major surface glycoprotein, gp63, of Leishmania*
578 *promastigotes.* J Exp Med, 1988. **168**(1): p. 279-92.
579 21. Guy, R.A. and M. Belosevic, *Comparison of receptors required for entry of Leishmania*
580 *major amastigotes into macrophages.* Infect Immun, 1993. **61**(4): p. 1553-8.
581 22. Sibley, L.D. and N.W. Andrews, *Cell invasion by un-palatable parasites.* Traffic, 2000.
582 **1**(2): p. 100-6.
583 23. Anastassiadis, T., et al., *Comprehensive assay of kinase catalytic activity reveals features*
584 *of kinase inhibitor selectivity.* Nat Biotechnol, 2011. **29**(11): p. 1039-45.
585 24. Morehead, J., I. Coppens, and N.W. Andrews, *Opsonization modulates Rac-1 activation*
586 *during cell entry by Leishmania amazonensis.* Infect Immun, 2002. **70**(8): p. 4571-80.
587 25. Hornbeck, P.V., et al., *PhosphoSitePlus, 2014: mutations, PTMs and recalibrations.*
588 Nucleic Acids Res, 2015. **43**(Database issue): p. D512-20.
589 26. Paul, J., et al., *TLR mediated GSK3beta activation suppresses CREB mediated IL-10*
590 *production to induce a protective immune response against murine visceral*
591 *leishmaniasis.* Biochimie, 2014. **107 Pt B**: p. 235-46.
592 27. Nandan, D., et al., *Myeloid cell IL-10 production in response to leishmania involves*
593 *inactivation of glycogen synthase kinase-3beta downstream of phosphatidylinositol-3*
594 *kinase.* J Immunol, 2012. **188**(1): p. 367-78.
595 28. Weirather, J.L., et al., *Comprehensive candidate gene analysis for symptomatic or*
596 *asymptomatic outcomes of Leishmania infantum infection in Brazil.* Ann Hum Genet,
597 2017. **81**(1): p. 41-48.
598 29. Srivastava, S., et al., *Leishmania expressed lipophosphoglycan interacts with Toll-like*
599 *receptor (TLR)-2 to decrease TLR-9 expression and reduce anti-leishmanial responses.*
600 Clin Exp Immunol, 2013. **172**(3): p. 403-9.
601

602

603 **Figures**

604 **Fig. 1. Host-targeted kinase inhibitors modulate infection of *Leishmania* in macrophages.**
605 **(A)** Invasion of *Leishmania* parasites is initiated by C3bi-opsonized promastigotes or
606 amastigotes interacting with complement receptors (*e.g.*, CR3) on macrophages, or amastigotes
607 entering macrophages via an IgG-mediated mechanism by binding to Fc receptors. **(B)** Four
608 representative stages of *Leishmania* infection in macrophages were studied: 30 min to
609 characterize initial parasite uptake, 3 h to assess the end of parasite uptake and trafficking to
610 the parasitophorous vacuole (PV), 24 h to visualize the transition from promastigote form to the
611 amastigote form, and 72 h to identify kinases needed for intracellular replication of amastigotes.
612 **(C)** Microscopy images showing that the multicolored fluorescence assay allows labeling of all
613 parasites (green channel) and parasites outside of macrophages (red channel). DAPI was used
614 to label cell nuclei (blue channel). See Materials and Methods for details on fluorescent labeling
615 and microscopy. **(D)** Cluster map showing the impact of a panel of 38 kinase inhibitors on
616 *Leishmania* infection in macrophages. *Leishmania* infection was quantified by phagocytic index -
617 the number of internalized particles per 100 mammalian cells, at 0.5, 3, 24, and 72 h post
618 infection. Phagocytic indices for kinase inhibitor-treated cells were normalized to the phagocytic
619 index of DMSO-treated control cells. Three independent experiments were performed. **(E)**
620 Correlations of normalized phagocytic index upon kinase inhibitor treatment between
621 amastigote-initiated infection via C3bi- and IgG-mediated mechanisms (top) and between
622 amastigote- and promastigote-initiated infection via C3bi-mediated mechanism (bottom).
623 Pearson correlation coefficient (r) is shown in each plot.

624

625 **Fig. 2. Host kinases regulate *Leishmania* infection through mechanisms independent of**
626 **phagocytosis. (A)** Workflow of using kinase inhibitor screen and machine learning algorithm to
627 identify host kinase regulators important for *Leishmania* infection in macrophages. **(B)** Left:

628 Venn diagrams showing the number of kinases predicted to modulate IgG-mediated uptake of
629 amastigotes and beads at different stages of infection. Right: black squares represent the
630 Pearson correlation coefficients calculated from the normalized phagocytic index upon kinase
631 inhibitor treatment between amastigote-initiated infection via C3bi- and IgG-mediated
632 mechanisms; green circles represent the p-values from hypergeometric test performed on KiR-
633 predicted kinases between amastigote and bead uptake via IgG-mediated mechanism; green
634 dashed line corresponds to p-value of 0.05. **(C)** Left: Venn diagrams showing the number of
635 kinases predicted to modulate C3bi-mediated uptake of promastigotes and beads at different
636 stages of infection. Right: black squares represent the Pearson correlation coefficients
637 calculated from the normalized phagocytic index upon kinase inhibitor treatment between
638 promastigote-initiated infection and bead uptake via a C3bi-mediated mechanism. Orange
639 circles represent the p-values from hypergeometric test performed on KiR-predicted kinases
640 between promastigote and bead uptake via C3bi-mediated mechanism. Orange dashed line
641 corresponds to p-value of 0.05. **(D)** Left: Venn diagrams showing the number of kinases
642 predicted to modulate C3bi-mediated uptake of amastigotes and beads at different stages of
643 infection. Right: black squares represent the Pearson correlation coefficients calculated from the
644 normalized phagocytic index upon kinase inhibitor treatment between amastigote-initiated
645 infection and bead uptake via C3bi-mediated mechanism. Brown circles represent the p-values
646 from hypergeometric test performed on KiR-predicted kinases between amastigote and bead
647 uptake via C3bi-mediated mechanism. Brown dashed line corresponds to p-value of 0.05. **(E)**
648 Phosphosignaling network built from the overlapping kinases predicted in IgG-mediated uptake
649 of amastigotes and beads at 3-hour time point. Kinases predicted by KiR are in green. **(F)**
650 Targeting the ERK pathway using a MEK inhibitor (trametinib) reduced macrophage uptake of
651 amastigotes via an IgG-mediated mechanism (left), as well as the phagocytosis of IgG-coated
652 beads (right). The phagocytic index, the number of intracellular amastigotes or beads per 100
653 macrophages, was calculated for each trametinib-treated biological replicate and normalized to

654 the DMSO-treated biological replicate (100%). Shown is the normalized phagocytic index at 3-
655 hour post internalization (n = 4 biological replicates for amastigotes; 3 biological replicates for
656 beads). One of trametinib's targets, MAP2K1/MEK1, is highlighted in dark green in (E).

657

658 **Fig. 3. Host kinases differentially regulate *Leishmania* promastigote and amastigote**
659 **infection in macrophages. (A)** Left: Venn diagrams showing the number of kinases predicted
660 to modulate C3bi-mediated uptake of promastigotes, amastigotes, and beads at different stages
661 of infection. Kinases predicted to regulate both promastigote and amastigote infection but not
662 bead uptake are listed. Right: black squares represent the Pearson correlation coefficients
663 calculated from the normalized phagocytic index upon kinase inhibitor treatment between
664 promastigote- and amastigote-initiated infection via C3bi-mediated mechanism; purple circles
665 represent the p-values from hypergeometric test performed on KiR-predicted kinases between
666 promastigote and amastigote infection via C3bi-mediated mechanism; purple dashed line
667 corresponds to p-value of 0.05. **(B)** Phosphosignaling network built from the kinases predicted
668 to exclusively regulate promastigote-initiated infection at 24 h post infection (labeled in
669 magenta), using the kinase-substrate phosphorylation database on PhosphoSitePlus® as the
670 background network.

671

672 **Fig. 4. Host kinases differentially regulate *Leishmania* infection via C3bi- and IgG-**
673 **mediated entry mechanisms. (A)** Left: Venn diagrams showing the number of kinases
674 predicted to modulate C3bi- and IgG-mediated uptake of amastigotes at different stages of
675 infection. Right: black squares represent the Pearson correlation coefficients calculated from the
676 normalized phagocytic index upon kinase inhibitor treatment between C3bi- and IgG-mediated
677 uptake of amastigotes; light blue circles represent the p-values from hypergeometric test
678 performed on KiR-predicted kinases between C3bi- and IgG-mediated uptake of amastigotes;

679 light blue dashed line corresponds to p-value of 0.05. **(B)** Left: Venn diagrams showing the
680 number of kinases predicted to modulate C3bi- and IgG-mediated uptake of beads at different
681 time points. Right: black squares represent the Pearson correlation coefficients calculated from
682 the normalized phagocytic index upon kinase inhibitor treatment between C3bi- and IgG-
683 mediated uptake of beads; gold circles represent the p-values from hypergeometric test
684 performed on KiR-predicted kinases between C3bi- and IgG-mediated uptake of beads; gold
685 dashed line corresponds to p-value of 0.05. **(C)** Phosphosignaling network built from the kinases
686 predicted to exclusively regulate amastigote-initiated infection via C3bi-mediated mechanism at
687 0.5 h post infection (labeled in blue), using the kinase-substrate phosphorylation database on
688 PhosphoSitePlus® as the background network.

689

690 **Supplemental Figures**

691 **Fig. S1. Correlations of normalized phagocytic index upon kinase inhibitor treatment**
692 **between different conditions. (A)** Correlation between amastigote and bead uptake via IgG-
693 mediated mechanism. **(B)** Correlation between promastigote and bead uptake via C3bi-
694 mediated mechanism. **(C)** Correlation between amastigote and bead uptake via C3bi-mediated
695 mechanism. **(D)** Correlation of bead uptake between IgG- and C3bi-mediated mechanisms.
696 Pearson correlation coefficient (r) is shown in each plot.

697

698 **Fig. S2. Phosphosignaling networks built from the overlapping kinases predicted in C3bi-**
699 **mediated uptake of promastigotes and beads.** Networks were built at 3 h (A) and 0.5 h (B)
700 post internalization. Kinases predicted by KiR are in orange.

701

702 **Supplemental Tables**

703 **Table S1. Normalized phagocytic indexes (with respect to DMSO (100%)) from kinase**
704 **inhibitor screens.** Three biological replicates were performed at each condition. This is a
705 Microsoft Excel workbook containing 5 spreadsheets.

706

707 **Table S2. List of kinases predicted by KiR.** This is a Microsoft Excel workbook containing 5
708 spreadsheets. Kinases predicted to inhibit or promote uptake/survival are in blue or red,
709 respectively.

710

Figure 1

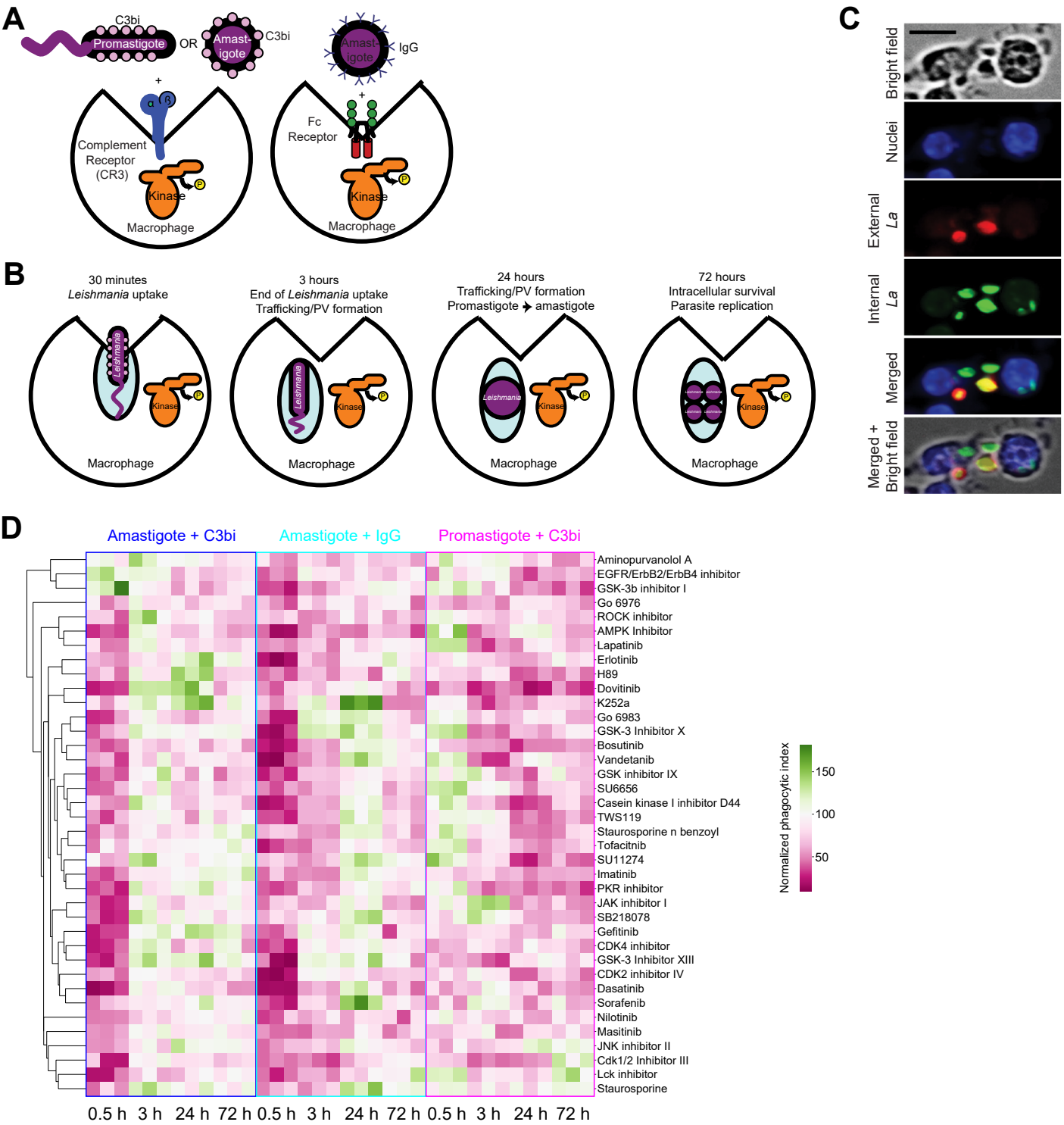
A
C3bi
Promastigote
OR
Amast-igote
C3bi
IgG
Complement Receptor (CR3)
Fc Receptor
Kinase
Macrophage
B
30 minutes
Leishmania uptake
3 hours
End of Leishmania uptake
Trafficking/PV formation
24 hours
Trafficking/PV formation
Promastigote → amastigote
72 hours
Intracellular survival
Parasite replication
C
Bright field
Nuclei
External La
Internal La
Merged
Merged + Bright field
D
Amastigote + C3bi
Amastigote + IgG
Promastigote + C3bi
Aminopurvanolol A
EGFR/ErbB2/ErbB4 inhibitor
GSK-3b inhibitor I
Go 6976
ROCK inhibitor
AMPK Inhibitor
Lapatinib
Erlotinib
H89
Dovitinib
K252a
Go 6983
GSK-3 Inhibitor X
Bosutinib
Vandetanib
GSK inhibitor IX
SU6656
Casein kinase I inhibitor D44
TWS119
Staurosporine n benzoyl
Tofacitnib
SU11274
Imatinib
PKR inhibitor
JAK inhibitor I
SB218078
Gefitinib
CDK4 inhibitor
GSK-3 Inhibitor XIII
CDK2 inhibitor IV
Dasatinib
Sorafenib
Nilotinib
Masitinib
JNK inhibitor II
Cdk1/2 Inhibitor III
Lck inhibitor
Staurosporine
0.5 h 3 h 24 h 72 h 0.5 h 3 h 24 h 72 h 0.5 h 3 h 24 h 72 h
Normalized phagocytic index
150
100
50
E
0.5 h
3 h
24 h
72 h
r=0.14
r=0.31
r=0.27
r=0.22
r=0.20
r=-0.066
r=-0.066
r=0.20
Amastigote + IgG
Amastigote + C3bi
Promastigote + C3bi

Figure 2

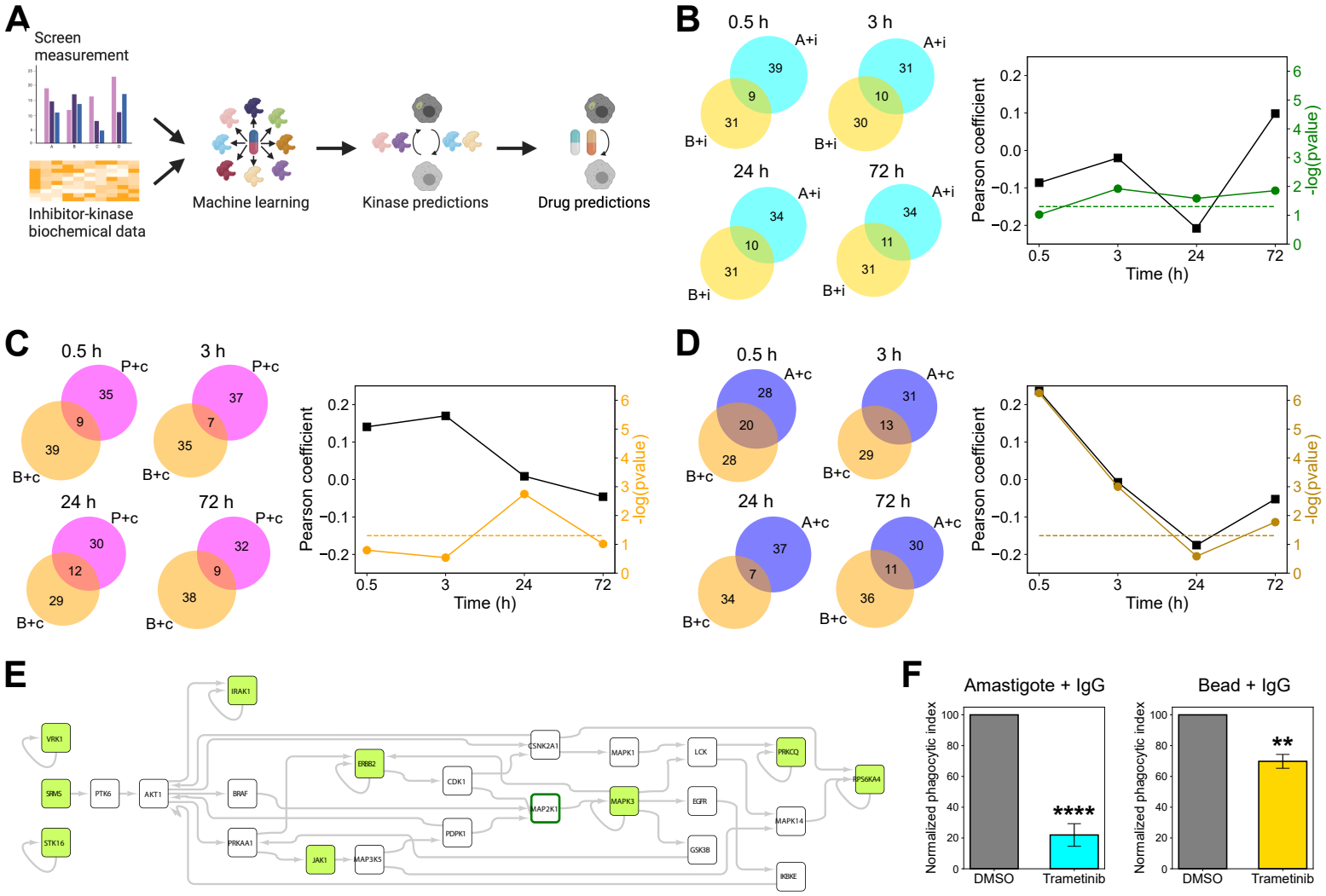
A
Screen measurement
Inhibitor-kinase biochemical data
Machine learning
Kinase predictions
Drug predictions
B
0.5 h
3 h
24 h
72 h
A+i
B+i
Pearson coefficient
-log(pvalue)
Time (h)
C
P+c
B+c
D
A+c
E
IRAK1
VRK1
SRM5
STK16
PTK6
AKT1
BRAF
PRKAA1
JAK1
MAP3K5
ERBB2
CDK1
PDPK1
CSNK2A1
MAP2K1
MAPK1
MAPK3
LCK
EGFR
GSK3B
PRKCQ
MAPK14
IKBKE
RPS6KA4
F
Amastigote + IgG
Bead + IgG
Normalized phagocytic index
DMSO
Trametinib
****
**

Figure 3

A

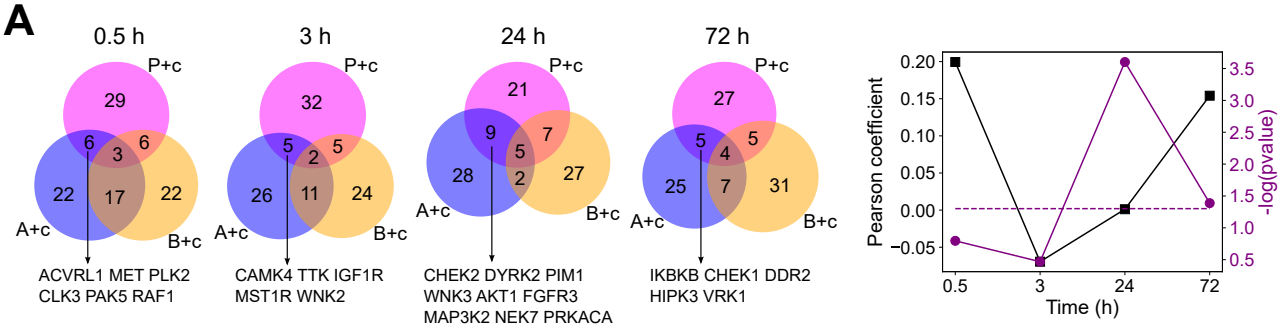
0.5 h
P+c
29
6
3
6
22
17
22
A+c
B+c
ACVRL1 MET PLK2
CLK3 PAK5 RAF1
3 h
P+c
32
5
2
5
26
11
24
A+c
B+c
CAMK4 TTK IGF1R
MST1R WNK2
24 h
P+c
21
9
7
5
28
2
27
A+c
B+c
CHEK2 DYRK2 PIM1
WNK3 AKT1 FGFR3
MAP3K2 NEK7 PRKACA
72 h
P+c
27
5
5
4
25
7
31
A+c
B+c
IKBKB CHEK1 DDR2
HIPK3 VRK1
Pearson coefficient
0.20
0.15
0.10
0.05
0.00
−0.05
-log(pvalue)
3.5
3.0
2.5
2.0
1.5
1.0
0.5
0.5
3
24
72
Time (h)

B

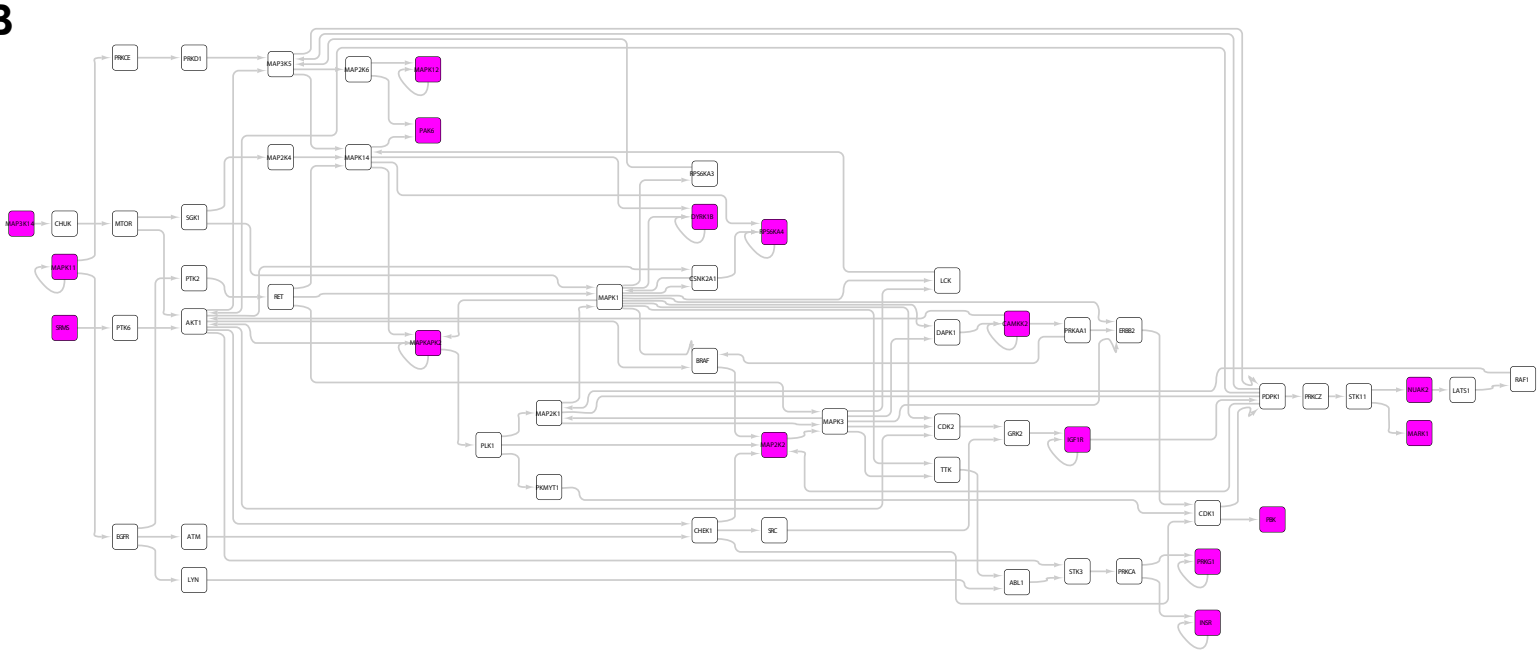
PRKCE
PRKD1
MAP3K5
MAP2K6
MAPK12
PAK6
MAP2K4
MAPK14
RPS6KA3
DYRK1B
RPS6KA4
MAP3K14
CHUK
MTOR
SGK1
MAPK11
PTK2
CSNK2A1
LCK
RET
MAPK1
SRM5
PTK6
AKT1
DAPK1
CAMKK2
PRKAA1
ERBB2
MAPKAPK2
BRAF
RAF1
PDPK1
PRKCZ
STK11
NUAK2
LATS1
MAP2K1
MAPK3
CDK2
GRK2
IGF1R
MARK1
PLK1
MAP2K2
TTK
NKMYT1
CDK1
PBK
EGFR
ATM
CHEK1
SRC
PRKG1
LYN
ABL1
STK3
PRKCA
INSR

Figure 4

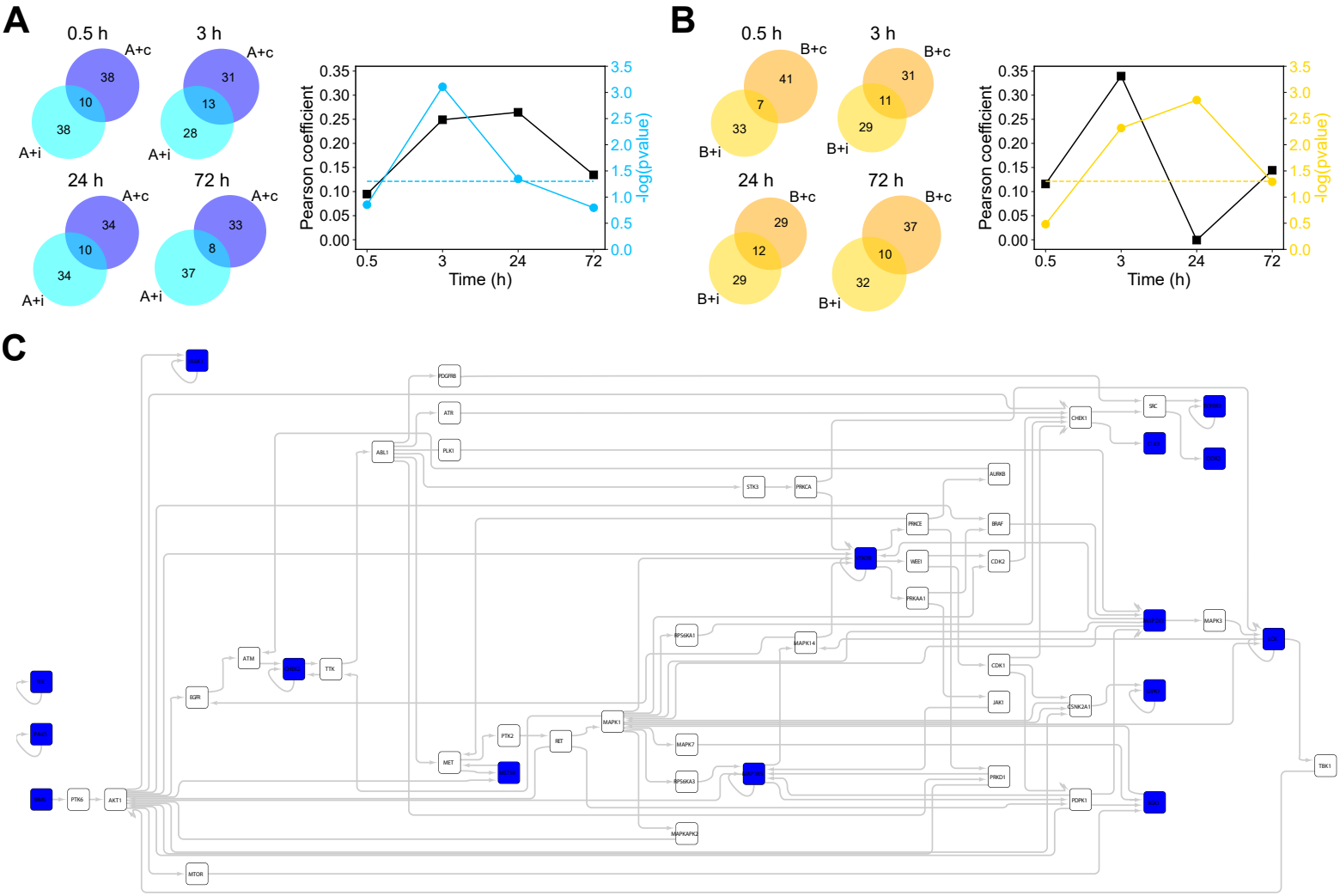
A
0.5 h
A+c
38
10
38
A+i
3 h
A+c
31
13
28
A+i
24 h
A+c
34
10
34
A+i
72 h
A+c
33
8
37
A+i
Pearson coefficient
-log(pvalue)
Time (h)
B
0.5 h
B+c
41
7
33
B+i
3 h
B+c
31
11
29
B+i
24 h
B+c
29
12
29
B+i
72 h
B+c
37
10
32
B+i
Pearson coefficient
-log(pvalue)
Time (h)
C
PDGFRB
ATR
PLK1
ABL1
STK3
PRKCA
AURKB
PRKCE
BRAF
WEE1
CDK2
PRKAA1
CHEK1
SRC
MAPK3
RPS6KA1
MAPK14
CDK1
JAK1
CSNK2A1
ATM
TTK
EGFR
MAPK1
PTK2
RET
MET
MAPK7
RPS6KA3
PRKD1
PDPK1
TBK1
PTK6
AKT1
MAPKAPK2
MTOR